European Review for Medical and Pharmacological Sciences 2019; 23: 11051-11061

# Effect of propofol on myocardial ischemia-reperfusion injury through MAPK/ERK pathway

H.-J. YAN[1], G.-Q. QI[2], Y. MA[3]

[1]Department of Anesthesiology, Chengyang People's Hospital, Qingdao, China
[2]Department of Anesthesiology, Urumqi First People's Hospital, Urumqi, China
[3]Department of Anesthesiology, The 970th Hospital of Chinese People's Liberation Army, Yantai, China

**Abstract. – OBJECTIVE: The aim of this study was to investigate the effects of propofol on myocardial ischemia-reperfusion injury (MIRI) and the mitogen-activated protein kinase (MAPK)/extracellular signal-regulated kinase (ERK) pathway.**

**MATERIALS AND METHODS: Primary cells were first isolated from rats. The effects of propofol on the apoptosis of primary myocardial cells and the expression of apoptosis-related proteins were detected via flow cytometry and Western blotting, respectively. Meanwhile, the effect of propofol on MIRI model after ischemia for 2 h and reperfusion for 24 h was detected as well. Subsequently, the effect of propofol on the activity of proteins in myocardial tissues was detected using transcriptome sequencing and VIPER method. The effect of propofol on myocardial tissues was detected via 2, 3, 5- triphenyl tetrazolium chloride (TTC) staining, hematoxylin-eosin (HE) staining, and Masson staining. Besides, the effect of propofol on myocardial function was detected using the BL-420F hemodynamic system. Propofol effect on the MAPK/ERK signaling pathway was determined via Western blotting *in vivo*. Finally, the effects of propofol on the content of serum lactate dehydrogenase (LDH), creatine kinase (CK), total superoxide dismutase (T-SOD), and malondialdehyde (MDA) were detected using relevant kits.**

**RESULTS: Propofol activated the MAPK/ERK signaling pathway in a dose-dependent manner in primary myocardial cells, which also reduced the apoptotic rate of myocardial cells. The results of TTC staining, HE staining, and Masson staining showed that propofol significantly reduced MIRI in a dose-dependent manner *in vivo*. ERK inhibitor PD-98059 could significantly reduce the cardioprotective effect of propofol. Propofol significantly decreased the content of serum LDH, CK, and MDA ($p<0.05$), while it increased the content of T-SOD ($p<0.05$). According to the hemodynamic study, statistically significant differences were observed in left ventricular systolic pressure (LVSP), maximal rate of the decrease of left ventricular pressure (-dp/dtmax), and left ventricular end-diastolic pressure (LVEDP) between propofol group and model group ($p<0.01$). The results of Western blotting revealed that propofol increased the protein expression level of p-ERK1/2 in a dose- and time-dependent manner *in vivo*. Furthermore, the expression level of p-ERK1/2 remarkably increased at 8 h after ischemia-reperfusion.**

**CONCLUSIONS: Propofol exerts a cardio-protective effect on MIRI through the MAPK/ERK pathway.**

*Key Words:*
Propofol, MAPK/ERK, Myocardial ischemia-reperfusion injury (MIRI).

## Introduction

Ischemic cardiomyopathy is a common cardiovascular disease with high morbidity and mortality rate in the world. It accounts for approximately 42% of the total cardiovascular diseases[1]. The prevention and treatment of myocardial ischemia-reperfusion injury (MIRI) play a key role in the treatment of coronary heart disease. Currently, such a pathological process has become a major clinical problem in the treatment of ischemic cardiomyopathy[2]. Previous studies have shown that the pathological mechanism of MIRI is very complicated. The widely-accepted theories of MIRI mainly include the impairment of myocardial energy metabolism, massive production of reactive oxygen species, the overload of calcium ion, neutrophil infiltration and vascular endothelial dysfunction. This may ultimately lead to apoptosis or necrosis of myocardial cells[3].

Extracellular signal-regulated kinase (ERK) is an important member of the mitogen-activated protein kinase (MAPK) family. Previous studies have indicated that ERK can regulate cell pro-

*Corresponding Author:* Yong Ma, BM; e-mail: mayong9618@163.com

liferation and differentiation. Activated ERK/MAPK will enter the nucleus to phosphorylate multiple transcription factors such as c-fos and serum response factor (SRF), thereby promoting the expressions of related genes[4]. Under the state of myocardial ischemia, the MAPK/ERK signaling pathway is activated to promote the expression of hypoxia-inducible factor 1 (HIF-1), eventually adapting to hypoxia. Current studies have found that the ERK1/2 signaling pathway plays a cardioprotective role in MIR. Moreover, the inhibition of the ERK1/2 signaling pathway promotes ischemia-reperfusion-induced myocardial apoptosis[5].

Propofol is mainly applied in anesthesia and sedation. According to pharmacological researches[6], other effects include anti-inflammation and inhibition of the production of pro-inflammatory cytokines and neutrophil infiltration. Clinical studies[7] have demonstrated that propofol can induce massive expression of oxidative stress biomarker heme oxygenase-1 (HO-1), thereby exerting an antioxidant effect. Propofol promotes cholesterol efflux through ABCA1 up-regulation, ultimately preventing endothelial cell inflammation and death caused by reactive oxygen species[8]. In addition, inhibits the damage caused by oxygen-glucose deprivation (OGD) in H9C2 cells, exerting a cardioprotective effect[9]. However, the mechanism of propofol in the prevention and treatment of myocardial injury has not been fully elucidated.

Propofol can increase the bioavailability of nitric oxide (NO) and up-regulate the expression level of endothelial nitric oxide synthase (eNOS) in human venous endothelial cells. This can eventually increase biosynthesis level of NO[10]. Moreover, propofol activates the ERK1/2 signaling pathway both at cellular and animal levels[11]. Therefore, it was hypothesized that propofol exerted a cardioprotective effect through the MAPK/ERK signaling pathway. In the present research, the cardioprotective effect of propofol and its effect on the MAPK/ERK signaling pathway were explored using classical models established *via* ligation of the left anterior descending artery and OGD model of primary myocardial cells.

## Materials and Methods

### Primary Myocardial Cell Culture

All animal operations were performed according to the Guidelines for the Care and Use of Laboratory Animals (NIH No. 85-23, revised in 1996). This investigation was approved by the Animal Ethics Committee of our hospital. Primary myocardial cells were isolated with collagenase II (Sigma-Aldrich, St. Louis, MO, USA) from the ventricle of Sprague-Dawley (SD) rats aged 1-3 days old. Briefly, ventricular tissues were cut into pieces and digested with 0.04% of collagenase II. The supernatant containing suspended cells was pre-plated for 1.5 h to remove non-myocardial cells. Subsequently, isolated myocardial cells were inoculated into cell culture plates (about $5\times10^4$ cells/cm$^2$), followed by culture in Dulbecco's Modified Eagle's Medium/Nutrient Mixture F-12 (DMEM/F-12) and HEPES (Hyclone, South Logan, UT, USA) containing 10% of fetal bovine serum (FBS; Gibco, Rockville, MD, USA) and 1% of penicillin-streptomycin (Solarbio, Beijing, China) in an incubator with 5% $CO_2$ at 37°C[12].

### OGD Cell Model

With dimethyl sulfoxide (DMSO) as a medium, propofol was dissolved in serum containing 10% FBS. In this study, all cells were divided into four groups, including high-dose propofol group (30 μM), medium-dose propofol group (20 μM), low-dose propofol group (10 μM), and model group. At 24 h after drug treatment, the medium was discarded and carefully rinsed with phosphate-buffered saline (PBS). Next, the solution was replaced with Krebs-Ringer bicarbonate buffer (KRB, 115 mM NaCl, 4.7 mM KCl, 2.5 mM $CaCl_2$, 1.2 mM $KH_2PO_4$, 1.2 mM $MgSO_4$, 24 mM $NaHCO_3$, and 10 mM HEPES, pH 7.4). After culture in a hypoxic environment (95% $N_2$ and 5% $CO_2$) for 6 h, the cells were cultured in DMEM containing 10% FBS in an incubator with 5% $CO_2$ and 95% air for 5 h for reoxygenation injury[13].

### Model of Myocardial Infarction and Determination of Cardiac Function in Rats

A total of 42 male SD rats weighing 180-200 g were fed in a specific pathogen-free animal house under the temperature of 25°C, a humidity of 45% and 12/12 h dark/light cycle. All rats were given free access to food and water. Propofol was dissolved in 0.5% sodium carboxyl methyl cellulose-Na (CMC-Na) solution. All 42 SD rats were randomly divided into 6 groups, including sham group, model group, 10 mg/kg propofol group, 15 mg/kg propofol group, 30 mg/kg propofol group, and 30 mg/kg propofol with 10 mg/kg PD-98059 group (a non-ATP competitive MEK inhibitor). In this study, the drug was injected through tail vein

1 h before modeling. Briefly, the ischemia-reperfusion model was established *via* ischemia for 30 min and reperfusion for 2 h. Rats were anesthetized with 1 g/kg urethane (Qingxi, Shanghai, China) and ventilated with a respirator (TKR-200C, Jiangxi, China) under the stroke volume of 12 mL/kg and frequency of 60 times/min. Subsequently, the chest was cut open by a left thoracic incision between the 2nd and 4th ribs. A 6-0 wire was threaded into the slip knot at 1/3 of the distal end of the left anterior descending artery. After that, the tube was placed between the ligature wire and myocardial tissues. Next, the coronary artery was blocked by tightening the suture line for ischemic injury. After ischemia for 2 h, the slip knot was loosened, followed by myocardial reperfusion for 24 h. Rats in sham group underwent the same operation as above except for ischemia-reperfusion[14].

Cardiac function was continuously monitored by electrocardiogram (ECG) throughout the ischemia-reperfusion period. Left ventricular systolic pressure (LVSP), left ventricular end-diastolic pressure (LVEDP), and maximal rate of the increase/decrease of left ventricular pressure (±dp/$dt_{max}$) were measured and recorded using the BL-420F hemodynamic system (Chengdu Technology Co., Ltd., Chengdu, China).

### Measurement of Myocardial Infarction Area

Myocardial infarction area was evaluated *via* 2,3,5- triphenyl tetrazolium chloride (TTC) staining. After reperfusion, the rats were executed immediately. Heart samples were taken out and sliced into 5 mm-thick sections along the apex to the bottom of the heart. After incubation with 1% TTC at 37°C for 15-20 min, the sections were photographed with a digital camera (Canon, Tokyo, Japan). The red part of the heart was stained with TTC, indicating the. survived tissues. Meanwhile, the white part indicated myocardial infarction. Finally, the infarction area was measured using the Image-Pro Plus software.

### Sequencing

The difference in gene expression induced by the intraperitoneal injection of Shenmai injection was explored using a high-throughput expression profile chip. At 2 h after intraperitoneal injection of Shenmai, total RNA was extracted from the tissues using TRIzol Reagent (Invitrogen, Carlsbad, CA, USA). Total extracted RNA was quantified using NanoDrop (Thermo Fisher, Waltham, MA, USA), and its integrity was evaluated by Bioanalyzer 2100 (Agilent, Santa Clara, CA, USA). 100 mg of total RNA was prepared into cRNA using the Affymetrix 3' IVT Express kit, followed by hybridization on an Affymetrix PrimeView Human Array at 45°C for 16 h according to the instructions of GeneChip 3' Array (Affymetrix, Santa Clara, CA, USA). Subsequently, the array was washed and stained on the Affymetrix FS-450 fluid station, followed by scanning on the Affymetrix GeneChip scanner. The raw data of CEL file were then imported into Partek Genomics Suite 6.6 software and the probe set was normalized using the Robust Multiarray Average method. (RMA). The differentially expressed genes were determined using one-way analysis of variance (ANOVA) and the *p*-value was corrected using the false discovery rate (FDR). In this study, normal myocardial tissues were used as control group, while myocardial tissues at 2 h after the injection of Shenmai were used as experimental group. This investigation was repeated 3 times[15].

### Prediction of Changes in Protein Activity Using VIPER Algorithm

The myocardial specific transcriptional regulatory network model was established using ARACNe based on 233 RNA-seq expression profile data obtained from the GEO database. Parameters of the ARACNe network were set as follows: bootstrap=100, $p<10^{-8}$, and DPI=0. The transcriptional regulatory network contained 1,623 TFs, 15,432 target genes, and 432,231 interactions. Based on the transcriptional regulatory network obtained above, the changes in protein activity affected by Shenmai injection were predicted using the VIPER algorithm provided by Bioconductor (https://www.bioconductor.org/packages/release/bioc/html/viper.html). Finally, the samples were randomly and uniformly scrambled for 1,000 times to estimate statistical significance[16].

### Apoptosis Detection

Changes in the apoptosis of myocardial cells after treatment were detected according to the instructions of Annexin V/propidium iodide (PI) double-staining kit. $5\times10^5$ cells were digested with trypsin and rinsed with PBS at 4°C twice. After centrifugation, the cells were re-suspended in 500 μL staining buffer. Then, 5 μL Annexin V-FITC and 5 μL PI dye were added followed by staining in the dark at 37°C for 15 min. Finally, the apoptosis of cells was detected using the Guava flow cytometer[11].

### Western Blotting

Cells were added with an appropriate amount of radio-immunoprecipitation assay (RIPA) lysis buffer and protease inhibitor phenylmethylsulfonyl fluoride (PMSF) (RIPA: PMSF = 100: 1) and mixed evenly (Beyotime, Shanghai, China). The cells were digested with trypsin, and the lysis buffer was added. The lysate was collected and transferred into an Eppendorf (EP) tube, followed by centrifugation at 14000 rpm and 4°C for 30 min using a refrigerated high-speed centrifuge. The supernatant of protein was collected and subjected to a heating bath at 95°C for 10 min for protein denaturation. Prepared protein samples were placed in a refrigerator at −80°C for subsequent use. The concentration of extracted protein was quantified using the bicinchoninic acid (BCA; Beyotime, Shanghai, China) method. Protein samples were separated by dodecyl sulfate, sodium salt-polyacrylamide gel electrophoresis (SDS-PAGE) under the constant pressure of 80 V for 2.5 h and transferred onto polyvinylidene difluoride (PVDF) membranes (Roche, Basel, Switzerland) using a semi-dry transfer method. Subsequently, PVDF membranes were immersed in Tris-Buffered Saline and Tween (TBST) containing 5% skim milk powder and shaken slowly for 1 h on a shaking table. After incubation with primary antibodies diluted with 5% skim milk powder, the membranes were rinsed with TBST for 3 times (10 min/time). Next, the membranes were incubated again with the corresponding secondary antibody at room temperature for 2 h, followed by rinsing again with TBST twice and Tris-buffered saline (TBS) once (10 min/time). Immunoreactive bands were exposed using the enhanced chemiluminescence (ECL) reagent in a dark room. The relative expression of the protein was analyzed using Image-Pro Plus v6 (Media Cybernetics, Silver Spring, MD, USA).

### HE Staining

The rats were first executed *via* dislocation at one time. Heart samples were isolated and treated with 4% paraformaldehyde/PBS (pH 7.4) at 4°C for 48 h. Then, the tissues were washed with running water, dehydrated with 70%, 80%, and 95% ethanol and treated with 100% ethanol. After that, the ethanol was removed with xylene. The tissues were embedded into paraffin (2 μm) and stained in strict accordance with the manufacturer's instructions of HE staining kit (Beyotime, Shanghai, China).

### Masson Staining

The rats were first executed *via* dislocation at one time. Heart samples were isolated and treated with 4% paraformaldehyde/PBS (pH 7.4) at 4°C for 48 h. Then the tissues were washed with running water, dehydrated with 70%, 80%, and 95% ethanol and treated with 100% ethanol. After that, the ethanol was removed with xylene. The tissues were embedded into paraffin (2 μm), deparaffinized, washed with water and air-dried. The nucleus was stained with reagent A (Masson's Trichrome staining kit, Shanghai Bogoo Biotechnology Co., Ltd., Shanghai, China) for 10 min and examined under a microscope, showing the blue color. After washing with water and dried air, the sections were treated with reagent B at room temperature for 15 min. Reagent B was then removed with reagent C. Reagent D and E were added for differentiation and staining for 10 s, respectively. After reagents were removed with reagent C, the sections were made transparent with 95% alcohol, anhydrous alcohol, and xylene, followed by sealing with neutral balsam. Finally, the sections were observed under a microscope.

### Measurement of Serum Content of Layered Double Hydroxide (LDH), CK, T-SOD, and MDA

At 24 h after reperfusion, blood samples were collected from the abdominal aorta and centrifuged at 1500 g and 4°C for 10 min to collect the serum. CK was measured at 520 nm, and LDH was detected at 450 nm, as previously described[26]. The T-SOD activity and the MDA content were quantitatively detected at 550 nm via Thiobarbituric acid (TBA) assay according to the manufacturer's instructions[27]. This investigation was repeated 3 times for each sample.

### Statistical Analysis

Statistical Product and Service Solutions (SPSS) 20.0 (SPSS, Chicago, IL, USA) was used for all statistical analysis. Three parallel groups were set for all experiments, which were repeated for 3 times. The results were expressed as mean ± standard deviation (SD). The *t*-test was adopted for intergroup comparison of differences. $p<0.05$ was considered statistically significant, and $p<0.01$ was considered extremely statistically significant.

## Results

### Propofol Reduced Hypoxia/Reoxygenation-Induced Apoptosis of Primary Myocardial Cells in a Dose-Dependent Manner

To evaluate the effect of propofol on hypoxia/reoxygenation-induced apoptosis of primary myocardial cells, flow cytometry was performed using the Annexin V/PI double-staining reagent. Results showed that propofol significantly reduced the apoptotic rate of primary myocardial cells in a dose-dependent manner (Figure 1A). Subsequently, the effect of propofol on the expression of apoptotic proteins was detected *via* Western blotting. The results revealed that propofol markedly reduced the protein expressions of active-caspase 3/pro-caspase 3 and Bax/Bcl-2 in a dose-dependent manner, and there were statistically significant differences ($p<0.05$) (Figures 1B, 1C and 1D).

### Effect of Propofol on MAPK/ERK Signaling Pathway in Primary Myocardial Cells

To search for proteins with significant changes in activity at 2 h after propofol treatment, 231 myocardial tissue gene expression profile data were downloaded from the GEO database. The myocardial tissue-specific transcriptional regulatory network was then constructed using the ARACNe algorithm. ARACNe algorithm is a theoretical prediction method to predict the relation between transcriptional regulatory factors and downstream genes of signaling proteins based on large-scale gene expression profile data. This method has proved to be a powerful method for VIPER analysis. Based on the VIPER

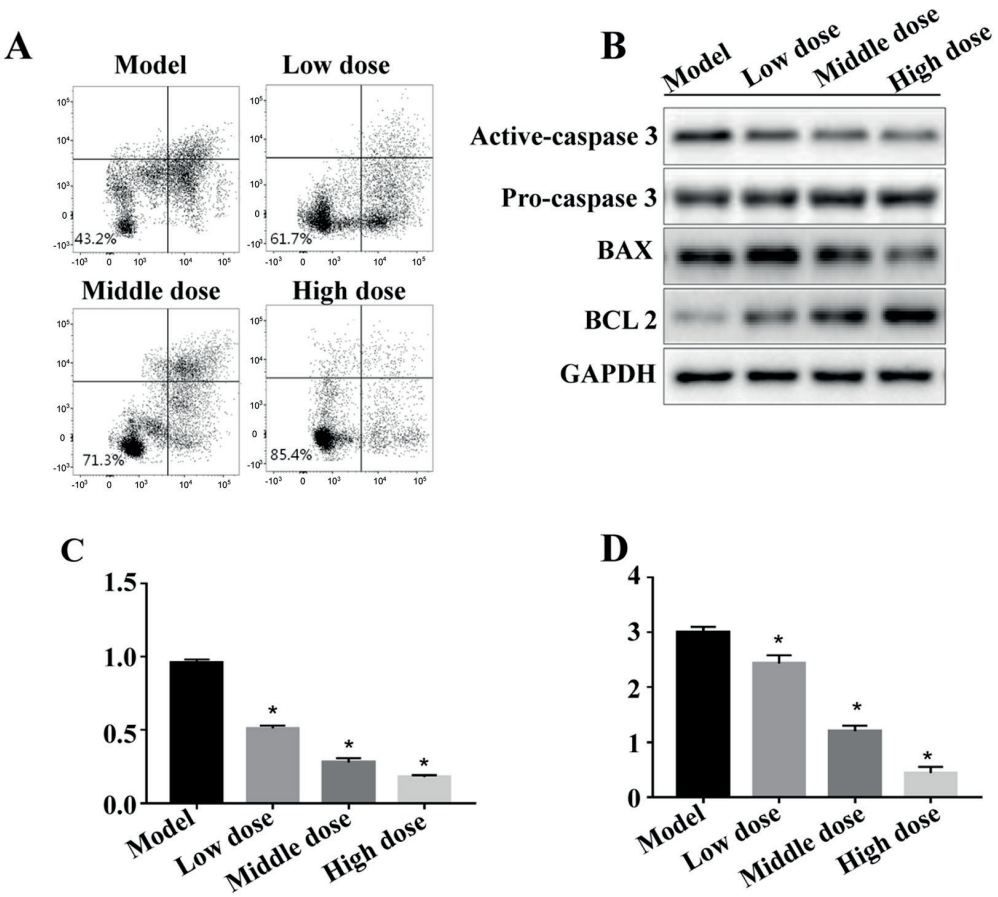


**Figure 1.** Propofol reduced hypoxia/reoxygenation-induced apoptosis of primary myocardial cells in a dose-dependent manner. **A,** Effect of propofol on hypoxia/reoxygenation-induced apoptosis of primary myocardial cells detected *via* flow cytometry. **B,** Effect of propofol on apoptotic proteins detected *via* Western blotting. **C-D,** Quantitative results of Western blotting. *$p<0.05$: drug treatment group *vs.* model group.

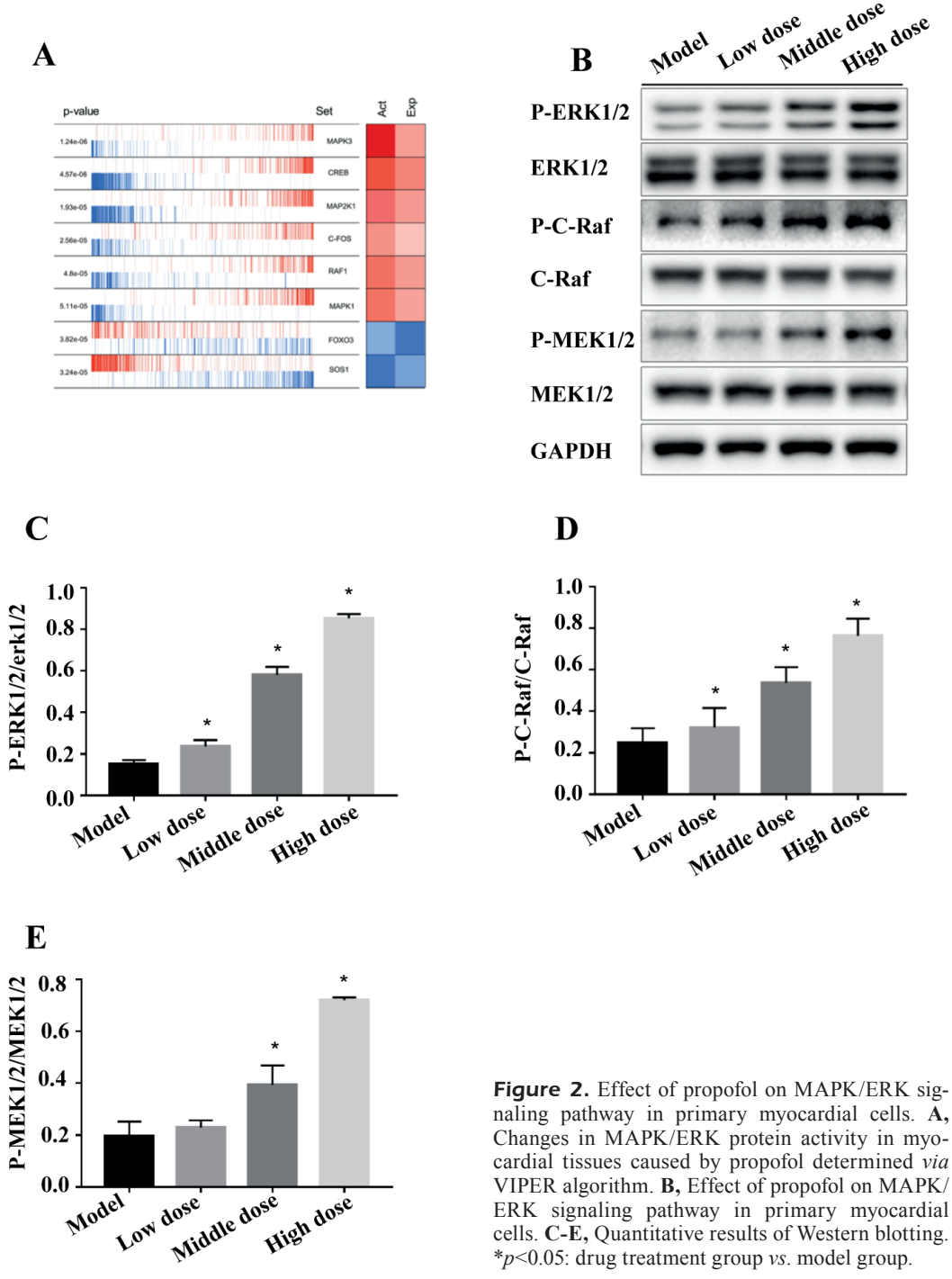


**Figure 2.** Effect of propofol on MAPK/ERK signaling pathway in primary myocardial cells. **A,** Changes in MAPK/ERK protein activity in myocardial tissues caused by propofol determined *via* VIPER algorithm. **B,** Effect of propofol on MAPK/ERK signaling pathway in primary myocardial cells. **C-E,** Quantitative results of Western blotting. **p*<0.05: drug treatment group *vs*. model group.

analysis, 6 proteins with significantly up-regulated activity (MAPK3, CREB, MAP2K1, C-FOS, RAF1, and MAPK1) and two proteins with markedly down-regulated activity (SOS1 and FOXO3) were obtained. In other words, the protein activity of MAPK/ERK signaling pathway was significantly up-regulated (Figure 2A). Furthermore, Western blotting indicated that the protein expression levels of p-ERK1/2, p-C-RAF, and p-MEK1/2 in the MAPK/ERK signaling pathway increased remarkably (Figures 2B, 2C, 2D and 2E).

### Propofol Reduced Ischemia-Reperfusion-Induced Myocardial Infarction Area in a Dose-Dependent Manner

Compared to model group, propofol markedly reduced ischemia-reperfusion-induced myocardial injury in a dose-dependent manner, showing a statistically significant difference ($p<0.05$). Compared to 30 mg/kg propofol group, ischemia-reperfusion-induced myocardial infarction area increased significantly in 30 mg/kg propofol + 10 mg/kg PD-98059 group ($p<0.05$) (Figures 3A and 3B).

### Effect of Propofol on Cardiac Function in IRI Rats

The effect of propofol on cardiac function in ischemia-reperfusion injury (IRI) rats was shown in Table I. Compared to sham group, LVSP, +dp/$dt_{max}$, and -dp/$dt_{max}$ were significantly declined, while LVEDP increased markedly in model group, showing statistically significant differences ($p<0.01$). Compared to model group, +dp/$dt_{max}$ increased significantly in 10 mg/kg propofol group, displaying a statistically significant difference ($p<0.05$). However, no statistically significant differences were observed in LVSP, -dp/$dt_{max}$ and LVEDP ($p>0.05$). Compared to model group, LVSP, +dp/$dt_{max}$, -dp/$dt_{max}$, and LVEDP were all significantly high in 15 mg/kg propofol group and 30 mg/kg propofol group ($p<0.01$). Moreover, LVSP, +dp/$dt_{max}$, -dp/$dt_{max}$, and LVEDP increased significantly in 30 mg/kg propofol + 10 mg/kg PD-98059 group when compared to 30 mg/kg propofol group ($p<0.01$).

### Effect of Propofol on Serum Biochemical Indexes in Rats

Compared to sham group, serum levels of LDH, CK, and MDA content increased significantly, while the content of T-SOD decreased markedly in model group ($p<0.01$). Compared with model group, serum levels of LDH, CK, and MDA content were significantly declined, whereas T-SOD was significantly elevated in 10 mg/kg propofol group ($p<0.05$). Moreover, serum levels of LDH, CK and MDA content were significantly declined, while T-SOD was significantly up-regulated in 15 mg/kg propofol group and 30 mg/kg propofol group when compared with model group ($p<0.01$). Furthermore, serum levels of LDH and CK in 30 mg/kg propofol with 10 mg/kg PD-98059 group was significantly higher than those of 30 mg/kg propofol group, and the differences were statistically significant ($p<0.05$).

### Effect of Propofol on Heart Tissues After IRI Determined Via HE Staining

Hematoxylin-eosin staining (HE) staining results were shown in Figure 4. In model group, the myocardial cells were arranged disorderly and were not of uniform size. Myocardial cell cytoplasm was stained non-uniformly, myocardial fibers were arranged loosely and disorderly, and the intercellular space was markedly widened. The myoplasm was stained non-uniformly as well. Meanwhile, degeneration and swelling occurred in some muscle fibers, with interstitial edema, erythrocyte leakage, and neutrophil infiltration (Figure 4A). 10 mg/kg of propofol significantly improved myocardial tissue structural damage. However, the inflammatory

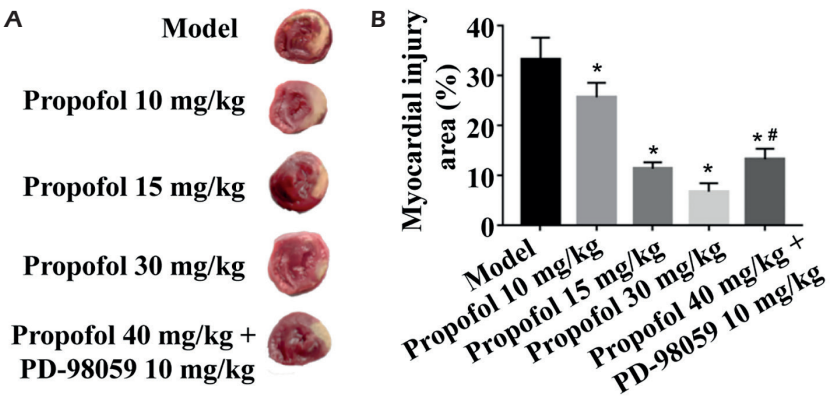


**Figure 3.** Propofol reduced ischemia-reperfusion-induced myocardial infarction area in a dose-dependent manner**. A,** Effects of propofol and ERK inhibitor on ischemia-reperfusion-induced myocardial infarction area. **B,** Quantitative results of effects of propofol and ERK inhibitor on ischemia-reperfusion-induced myocardial infarction area. *$p<0.05$: drug treatment group *vs.* model group, #$p<0.05$: 30 mg/kg propofol with 10 mg/kg PD-98059 group *vs.* 30 mg/kg propofol group.

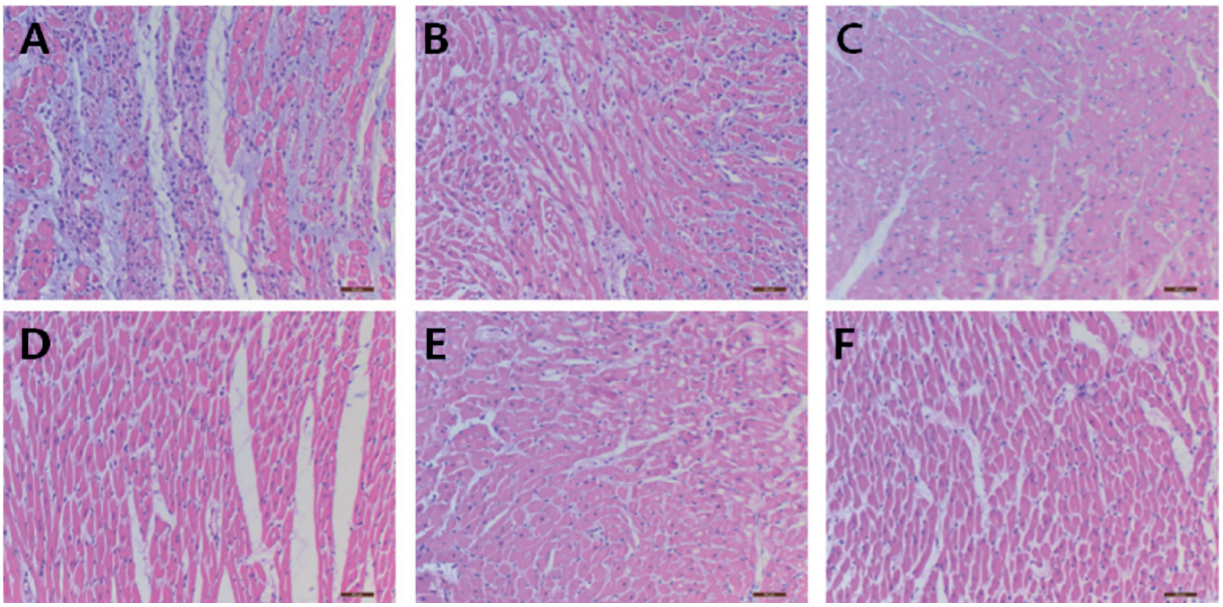


**Figure 4.** Effect of propofol on heart tissues after IRI determined *via* HE staining (magnification ×20). ***A,*** Model group, **B,** 10 mg/kg propofol group, **C,** 15 mg/kg propofol group. **D,** 30 mg/kg propofol group. **E,** 30 mg/kg propofol with 10 mg/kg PD-98059 group. **F,** sham group.

cell infiltration could still be observed (Figure 4B). 15 mg/kg of propofol showed a certain protective effect on the myocardium, while vacuolar degeneration could still be found in myocardial cells (Figure 4C). 30 mg/kg of propofol exerted a significantly better protective effect on the myocardium. Moreover, it could be observed that myocardial cells were arranged orderly and stained uniformly, and the intercellular boundary was clear without interstitial edema and neutrophil infiltration (Figure 4D). Vacuolar degeneration occurred in some myocardial cells in 30 mg/kg of propofol with 10 mg/kg of PD-98059 group as well (Figure 4E). In sham group, myocardial cells had normal size and morphology, and they were arranged orderly with clear intercellular boundary. However, myocardial tissue fibers and nuclei were stained uniformly, and the fibers were arranged orderly and connected closely. In addition, no infarction lesions were observed (Figure 4F).

### *Effect of Propofol on Heart Tissues After IRI Determined Via Masson Staining*

Myocardial fibrosis after myocardial infarction is one of the major causes of ventricular remodeling and cardiac dysfunction. The imbalance between synthesis and degradation of myocardial fiber collagen leads to myocardial rigidity and decline in heart compliance. This may affect cardiac systolic and diastolic functions, which can also cause a diminished cardiac function and even heart failure. According to the results of Masson staining (Figure 5), normal myocardial tissues were replaced with large-area fibrotic tissues in model group, and myocardial interstitial collagen was significantly proliferated. Meanwhile, the myocardial bundle was separated and wrapped with a large number of blue-stained fibrous connective tissues in a grid shape. Propofol significantly reduced the level of myocardial fibrosis in the rat model of myocardial infarction in a dose-dependent manner, thereby protecting the myocardium. In 30 mg/kg propofol with 10 mg/kg of PD-98059 group, blue-stained fibrosis could still be observed in some myocardial tissues.

### *Effect of Propofol on MAPK/ERK Signaling Pathway in Myocardial Tissues*

After treatment with propofol in different doses for 24 h, the protein level of p-ERK1/2 increased in a dose-dependent manner ($p<0.05$) (Figures 6A and 6C). Furthermore, 30 mg/kg of propofol markedly up-regulated the protein expression of p-ERK1/2 at 8 h after reperfusion (Figures 6B and 6D).

## Discussion

Coronary heart disease is the most common fatal disease in the world, with 3.8 million men

and 3.4 million women deaths every year. After acute myocardial infarction, early and successful myocardial reperfusion in thrombolytic therapy or percutaneous coronary intervention can significantly reduce the myocardial infarction area caused by acute myocardial infarction. This is also the most effective strategy to improve clinical outcomes. However, recovering blood supply to ischemic myocardium can induce myocardial injury. This phenomenon is known as myocardial reperfusion injury, which can reduce the beneficial effects of myocardial blood supply recovery. Animal experiments have suggested that myocardial infarction area caused by non-recovery of blood supply accounts for about 70% during myocardial infarction. The myocardial infarction area can be reduced to at least 5% by recovering the blood supply and applying cardioprotective drugs. However, it will still be about 30-40% under ischemia-reperfusion without the application of protective drugs. Such a form of myocardial injury can induce myocardial cell death and increase the infarction area. The mortality rate after acute myocardial infarction is close to 10%, meanwhile, the incidence rate of heart failure after acute myocardial infarction is almost 25%[18].

In the present study, our results revealed that propofol could reduce the apoptotic rate of myocardial cells in a dose-dependent manner in hypoxia/reoxygenation-induced primary myocardial cell injury. Meanwhile, it could also significantly increase the expression levels of key proteins (p-ERK1/2, p-MEK1/2 and p-C-RAF) in the MAPK/ERK signaling pathway in a dose-dependent manner. In the *in vivo* myocardial injury model induced by ischemia for 2 h and reperfusion for 24 h, propofol reduced myocardial infarction area in a dose-dependent manner and up-regulated the protein expression level of p-ERK1/2 in a dose- and time-dependent manner. 10 mg/kg of PD-98059 (an ERK inhibitor) could significantly reverse the cardio-protective effect of propofol. The above results indicated that the cardioprotective effect of propofol in IRI might be realized by activating the MAPK/ERK signaling pathway. In addition, 10 mg/kg of PD-98059 did not completely eliminate the cardioprotective effect of propofol. This indicated that the cardio-protective effect of propofol was not completely realized through the MAPK/ERK signaling pathway. According to the results of hemodynamic studies, pre-administration of 15 mg/kg propofol is able to improve the de terioration of cardiac function in rats due to IRI. Enzymes routinely measured in clinical laboratories are used to diagnose and monitor myocardial infarction, including CK and LDH. They have been proved to be highly expressed in myocardial tissues. Therefore, the activity of measurable serum enzymes will be significantly elevated in the case of death of a relatively small part of

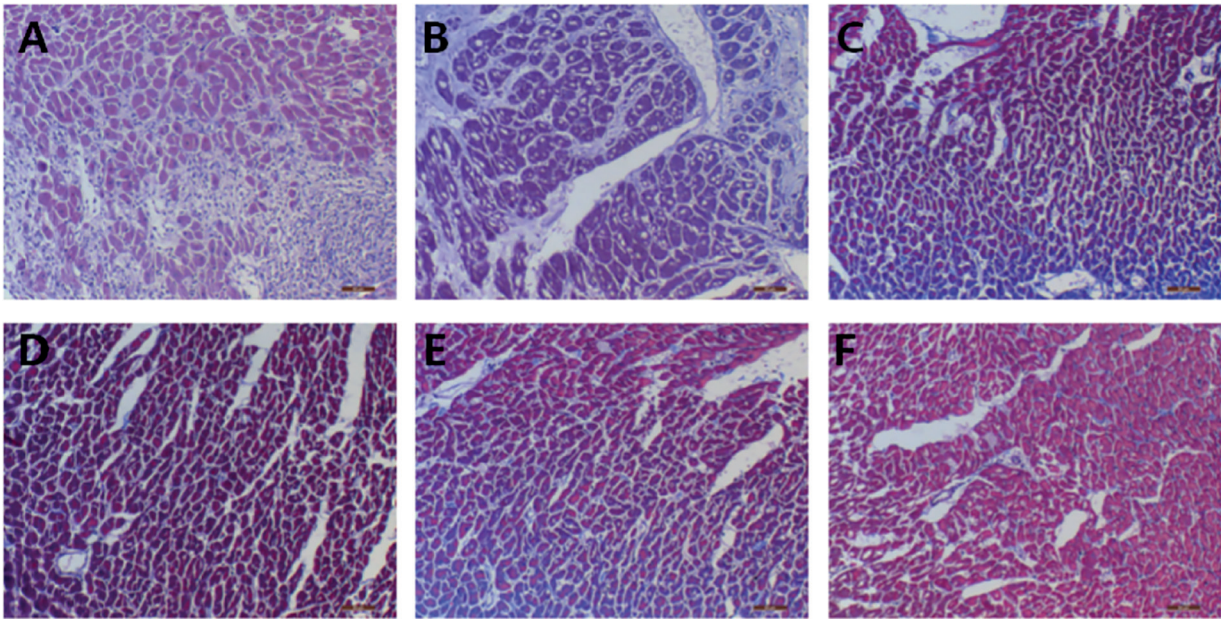


**Figure 5.** Effect of propofol on heart tissues after IRI determined *via* Masson staining (magnification × 20). ***A,*** Model group. ***B,*** 10 mg/kg propofol group. **C,** 15 mg/kg propofol group. **D,** 30 mg/kg propofol group. **E,** 30 mg/kg propofol with 10 mg/kg PD-98059 group. **F,** sham group.

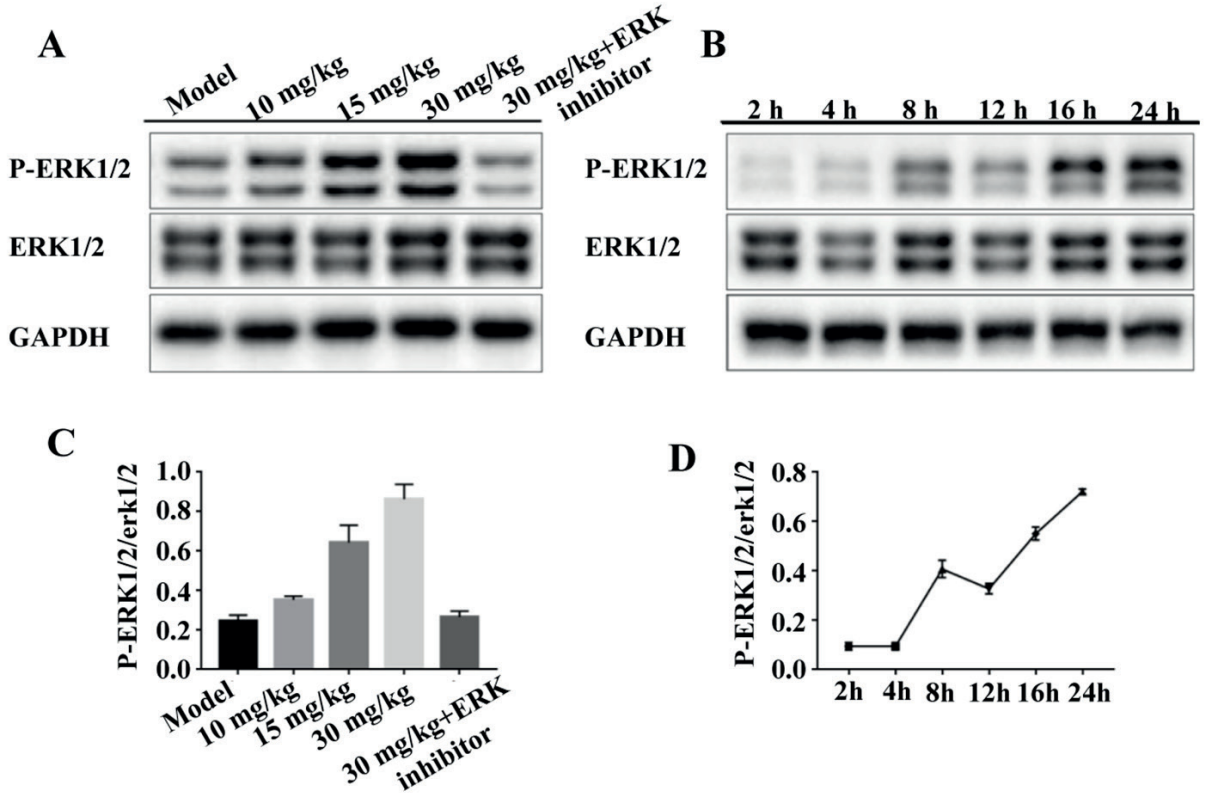


***Figure 6.*** Effect of propofol on MAPK/ERK signaling pathway in myocardial tissues. **A,** Effect of different doses of propofol on MAPK/ERK signaling pathway. **B,** Effect of propofol on MAPK/ERK signaling pathway in a time-dependent manner. **C,** The relative protein expression of p-ERK1/2/erk1/2 in a dose-dependent manner. **D,** The relative protein expression of p-ERK1/2/erk1/2 in a time-dependent manner. *$p$<0.05 drug treatment group *vs.* model group, **$p$<0.05: drug treatment group *vs.* model group, #$p$<0.05: 30 mg/kg propofol with 10 mg/kg PD-98059 group *vs.* 30 mg/kg propofol group

the tissues. High-level CK and LDH in heart tissues also indicate the emergence of myocardial infarction. Serum levels of LDH and CK in model group were significantly higher compared to propofol groups, indicating that myocardial cell injury was markedly alleviated[19].

MAPK is a superfamily of serine/threonine kinases, including ERK, JNK, and p38. All of these kinases are mainly involved in regulating the activation of nuclear transcription factors in cell proliferation, differentiation, and apoptosis. In the present work, we found that propofol exerted a cardioprotective effect through the ERK signaling pathway[20]. Furthermore, treatment with propofol for at least 8-12 h could phosphorylate ERK and increase the phosphorylation level of ERK in a time-dependent manner.

## Conclusions

Propofol exerts a cardioprotective effect through the MAPK/ERK signaling pathway. However, the reason for the activation of the MAPK/ERK signaling pathway by propofol remains to be further explored.

### Conflict of Interests

The Authors declare that they have no conflict of interests.

## References

1) Li GM, Zhang CL, Rui RP, Sun B, Guo W. Bioinformatics analysis of common differential genes of coronary artery disease and ischemic cardiomyopathy. Eur Rev Med Pharmacol Sci 2018; 22: 3553-3569.

2) Kohlhauer M, Dawkins S, Costa ASH, Lee R, Young T, Pell VR, Choudhury RP, Banning AP, Kharbanda RK; Oxford Acute Myocardial Infarction (OxAMI) Study, Saeb-Parsy K, Murphy MP, Frezza C, Krieg T, Channon KM. Metabolomic profiling in acute ST-segment-elevation myocardial infarction identifies succinate as an early marker of human ischemia-reperfusion injury. J Am Heart Assoc 2018; 7. pii: e007546.

3) Epelman S, Liu PP, Mann DL. Role of innate and adaptive immune mechanisms in cardiac injury and repair. Nat Rev Immunol 2015; 15: 117-129.

4) Thiel G, Rossler OG. Resveratrol stimulates c-Fos gene transcription via activation of ERK1/2 involving multiple genetic elements. Gene 2018; 658: 70-75.

5) Murphy E, Steenbergen C. Mechanisms underlying acute protection from cardiac ischemia-reperfusion injury. Physiol Rev 2008; 88: 581-609.

6) Vasileiou I, Xanthos T, Koudouna E, Perrea D, Klonaris C, Katsargyris A, Papadimitriou L. Propofol: a review of its non-anaesthetic effects. Eur J Pharmacol 2009; 605: 1-8.

7) Wang HH, Zhou HY, Chen CC, Zhang XL, Cheng G. Propofol attenuation of renal ischemia/reperfusion injury involves heme oxygenase-1. Acta Pharmacol Sin 2007; 28: 1175-1180.

8) Ma X, Li SF, Qin ZS, Ye J, Zhao ZL, Fang HH, Yao ZW, Gu MN, Hu YW. Propofol up-regulates expression of ABCA1, ABCG1, and SR-B1 through the PPARgamma/LXRα signaling pathway in THP-1 macrophage-derived foam cells. Cardiovasc Pathol 2015; 24: 230-235.

9) Wang B, Shravah J, Luo H, Raedschelders K, Chen DD, Ansley DM. Propofol protects against hydrogen peroxide-induced injury in cardiac H9c2 cells via Akt activation and Bcl-2 up-regulation. Biochem Biophys Res Commun 2009; 389: 105-111.

10) Oliveira-Paula GH, Lacchini R, Pinheiro LC, Ferreira GC, Luizon MR, Garcia WNP, Garcia LV, Tanus-Santos JE. Endothelial nitric oxide synthase polymorphisms affect the changes in blood pressure and nitric oxide bioavailability induced by propofol. Nitric Oxide 2018; 75: 77-84.

11) Titus HE, López-Juárez A, Silbak SH, Rizvi TA, Bogard M, Ratner N. Oligodendrocyte RasG12V expressed in its endogenous locus disrupts myelin structure through increased MAPK, nitric oxide, and notch signaling. Glia 2017; 65: 1990-2002.

12) Shen M, Wang L, Guo X, Xue Q, Huo C, Li X, Fan L, Wang X. A novel endoplasmic reticulum stress-induced apoptosis model using tunicamycin in primary cultured neonatal rat cardiomyocytes. Mol Med Rep 2015; 12: 5149-5154.

13) Raval AP, Dave KR, Prado R, Katz LM, Busto R, Sick TJ, Ginsberg MD, Mochly-Rosen D, Pérez-Pinzon MA. Protein kinase C delta cleavage initiates an aberrant signal transduction pathway after cardiac arrest and oxygen glucose deprivation. J Cereb Blood Flow Metab 2005; 25: 730-741.

14) Sonne DP, Engstrom T, Treiman M. Protective effects of GLP-1 analogues exendin-4 and GLP-1(9-36) amide against ischemia-reperfusion injury in rat heart. Regul Pept 2008; 146: 243-249.

15) Perez MV, Pavlovic A, Shang C, Wheeler MT, Miller CL, Liu J, Dewey FE, Pan S, Thanaporn PK, Absher D, Brandimarto J, Salisbury H, Chan K, Mukherjee R, Konadhode RP, Myers RM, Sedehi D, Scammell TE, Quertermous T, Cappola T, Ashley EA. Systems genomics identifies a key role for hypocretin/orexin Receptor-2 in human heart failure. J Am Coll Cardiol 2015; 66: 2522-2533.

16) Alvarez MJ, Shen Y, Giorgi FM, Lachmann A, Ding BB, Ye BH, Califano A. Functional characterization of somatic mutations in cancer using network-based inference of protein activity. Nat Genet 2016; 48: 838-847.

17) Vermes I, Haanen C, Steffens-Nakken H, Reutelingsperger C. A novel assay for apoptosis. Flow cytometric detection of phosphatidylserine expression on early apoptotic cells using fluorescein labelled Annexin V. J Immunol Methods 1995; 184: 39-51.

18) González-Montero J, Brito R, Gajardo AI, Rodrigo R. Myocardial reperfusion injury and oxidative stress: therapeutic opportunities. World J Cardiol 2018; 10: 74-86.

19) Lu S, Tang Y, Ding Y, Yu M, Fu S, Zhu B. [Effects of electroacupuncture on the expression of adenosine receptors in the heart tissue of myocardial ischemia rats]. Zhongguo Zhen Jiu 2018; 38: 173-179.

20) Zhang Q, Lu L, Liang T, Liu M, Wang ZL, Zhang PY. MAPK pathway regulated the cardiomyocyte apoptosis in mice with post-infarction heart failure. Bratisl Lek Listy 2017; 118: 339-346.